Interplay between plasmons and the band structure for the Mo(112) surface

I. N. Yakovkin
Institute of Physics, National Academy of Sciences of Ukraine, Prospect Nauki 46, Kiev UA-03039, Ukraine

Jiandi Zhang
Department of Physics, Florida International University, University Park, Miami, Florida 33199

P. A. Dowben
Department of Physics and Astronomy and the Center for Materials Research and Analysis, Behlen Laboratory of Physics, University of Nebraska-Lincoln, Lincoln, Nebraska 68588-0111

(Received 22 September 2000; published 27 February 2001)

Recent photoemission and inverse photoemission results for the Mo(112) surface are discussed in the framework of the calculated band structure. For the Mo(112) surface, the main photoemission features combine contributions from both the surface and the bulk. Except for those photon energies near to excitations of the bulk and multipole surface plasmons, the comparison of the bulk band structure, along the k points normal to the surface, shows a good agreement with photoemission spectra in the position of the critical points. The dominant surface states at $\bar{\Gamma}$ are found to have the a_1 symmetry, while the band along $\bar{\Gamma}$-$\bar{Y}$ at about 0.8 eV binding energy is found to be odd with respect to the $\bar{\Gamma}$-$\bar{X}$ mirror plane. The surface-induced enhancement of photoemission—the surface photoeffect—is indicated and is shown to be responsible for dramatic changes in the spectra when the photon energy falls into the region of the multipole surface plasmons.

DOI: 10.1103/PhysRevB.63.115408 PACS number(s): 68.35.Bs, 73.20.At

I. INTRODUCTION

Photoemission is one of the major experimental tools for investigation of the surface electronic structure (along with inverse photoemission and more recently scanning-tunneling spectroscopy). The mapping of the surface band structure can be facilitated by enhancing the surface sensitivity of photoemission. In one approach, enhanced surface sensitivity in photoemission can be gained due to the resonant light absorption at the surface, that is, ''optical'' surface photoeffect.[1–7] The surface photoeffect is closely related to the excitation and the subsequent decay of the multiple surface plasmons, or multipole mode.[8–13] This mechanism of the enhancement of the surface photoemission is widely recognized and has been reported for clean surfaces and thin films of simple metals.[3,11,14,15]

The mapping of the bulk band structure, using photoemission techniques,[7,16–18] can be facilitated by enhanced cross section (and therefore more intense peaks in the photoemission spectra) through the Coster-Kronig resonant optical transitions, as allowed by the photoemission selection rules. Identification of the bands, however, is complicated by surface and adsorbate umklapp processes[19–21] and surface reconstructions, in particular, well known to occur with molybdenum surfaces.[22–41] The surface photoeffect can further complicate the identification of the bulk bands by the normal photoemission technique by making both height and position of the spectral peaks dependent upon photon energy. These complications might result in an ambiguous interpretation of experimental data in absence of calculated band structure along the relevant directions in the bulk Brillouin zone.

The aim of the present work is the elucidation of the nature of the photoemission spectra and their relation to the electronic structure of the Mo(112) surface. We will show that with Mo(112), almost all the photoemission features combine contributions from both the surface and the bulk. To illustrate this suggestion, here we undertake an analysis of the angle-resolved photoemission (ARPES) and inverse photoemission (IPES) studies of the band structure, which have been partly published elsewhere,[22] and model linear augmented plane wave (LAPW) film calculations of the electronic structure for a free monolayer and for a three-layer slab simulating the Mo(112) surface. Calculations of the bulk band structure along the normal to the surface is also presented and compared with band dispersion found from the wave vector dependence ($k_\perp$-dependent) photoemission spectra along the surface normal.

II. EXPERIMENTAL AND CALCULATIONAL TECHNIQUES

The IPES and the low-energy electron diffraction (LEED) experiments were undertaken separately from the photoemission using an apparatus as described elsewhere.[22,42] The photoemission (ARPES) experiments, with a resolution between 0.10 and 0.25 eV, were carried out at the Synchrotron Radiation Center in Stoughton, Wisconsin in an ultrahigh vacuum (UHV) chamber employing a hemispherical electron energy analyzer with an angular acceptance of $\pm 1°$, which has also been described elsewhere.[43] The photoelectrons were collected with emission angles defined with respect to the surface normal.

The crystallographic order of the Mo(112) surface was verified by LEED and scanning tunneling microscopy (STM) and the absence of surface contamination by photoemission as the sample was prepared using established procedures.[22] The surface of the Mo(112) crystal was cleaned by repeated annealing in oxygen and electron bombardment (flashing)

 ©2001 The American Physical Society

and the crystal temperature was monitored with a W-5% Re W-26% Re thermocouple with an accuracy of ±5 K. Exposure of the Mo(112) crystal to oxygen was controlled with the use of a standard UHV leak valve.

Momentum conservation can be used, in principle, to determine the energy band dispersion relation with respect to the wave vector. The wave vector component parallel to the surface ($k_{\|}$) can be derived from the kinetic energy and the emission angle

$$k_{\|} = (2m/\hbar^2)^{1/2} E_{\mathrm{kin}} \sin\theta, \tag{1}$$

where, for IPES, E_{kin} is the kinetic energy of the incident electrons and θ is the incidence angle relative to normal incidence and, for photoemission, E_{kin} is the kinetic energy of the emitted photoelectron and θ is the emission angle relative to the surface normal. The perpendicular component of the crystal wave vector ($k_{\perp}$), however, is not conserved across the solid vacuum interface because of the crystal truncation at the surface. Thus, the perpendicular wave vector in the crystal can be determined using

$$k_{\perp} = \frac{-2m}{\hbar^2}[E_{\mathrm{kin}}[\cos(\theta)]^2 + U_{\mathrm{in}}]^{1/2}, \tag{2}$$

where θ is the emission angle of the photoelectron or the incident angle of the electron in inverse photoemission and U_{in} is the inner potential of the solid, which can be defined as approximately the width of the occupied part of the conduction band plus the work function.[16,44]

The band structures were calculated by the scalar relativistic all-electron LAPW method for thin films,[45–47] which explores a single (not periodically repeated) slab of several monolayers of thickness to simulate both surface and bulk contributions. In the interior of the slab, the potential is defined in the muffin-tin (MT) form, while in the vacuum region the potential depends only on z coordinate (that is, normal to the surface). Discrete k_z values, required for the expansion of the wave function into symmetrized plane waves in the interstitial region, are defined in accordance to the film thickness, while the basis functions in vacuum are obtained by inward numerical integration with the energy parameter chosen near the Fermi level.

In the present work, the self-consistent ''warped'' MT potential was recalculated for each iteration taking into account the redistribution of all core electrons. Corrections to the muffin-tin potential in the interstitial and vacuum regions were included through the Fourier expansion of charge densities,[47] while less important nonspherical corrections to the potential inside muffin-tin spheres were neglected. The exchange-correlation potential was adopted in the local density approximation form using the improved Wigner interpolation formula.[46] The number of basis functions was adjusted to provide 1 mRy convergence for the bands near E_F. Density of states (DOS) were calculated using the triangular integration method.[48]

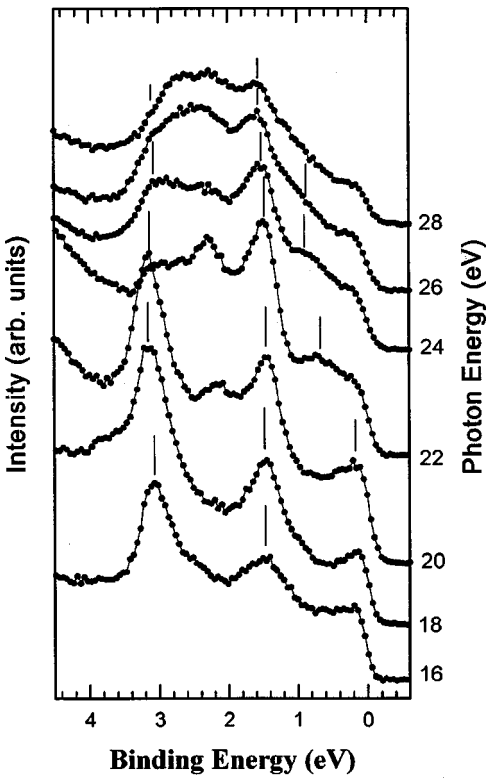

FIG. 1. The photoemission spectra taken at normal emission ($k_{\|}=0$) for photon energies 10–30 eV.

III. SURFACE BANDS NEAR E_F

The dependence of the normal-emission photoemission spectra upon photon energy (Figs. 1 and 2) results in significant changes in shape and intensity of all bands. The peak positions also strongly depend on photon energy except for those bands at approximately 3 and 1.5 eV binding energy (Fig. 3), for which $k_{\perp}$ is weaker. When the binding energies do not change with photon energy (no dependence upon the wave vector normal to the surface $k_{\perp}$), it indicates conservation of two dimensionality of state and suggests surface sensitivity. The fact that the states at approximately 3 and 1.5 eV binding energy are affected by small amounts of contamination provides further indication that these bands have some surface weight. None of the bands exhibiting surface sensitivity (and imperfect conservation of two dimensionality of state) appear to fall in a gap of the calculated bulk band structure (see below) and are, therefore, surface resonances rather than surface states.

Shown in Fig. 4 are the results of the band calculations for the Mo(112) monolayer [solid curves are the bands that have the z-reflection (even) symmetry while dashed lines are the odd states] and experimental photoemission and inverse photoemission data (partly published elsewhere[22]) for the surface-sensitive states (denoted by the dotted lines). The binding energies were plotted against the component of the wave vector parallel to the surface determined according to Eq. (1). The right panel of Fig. 4 presents the calculated DOS for the Mo(112) monolayer.

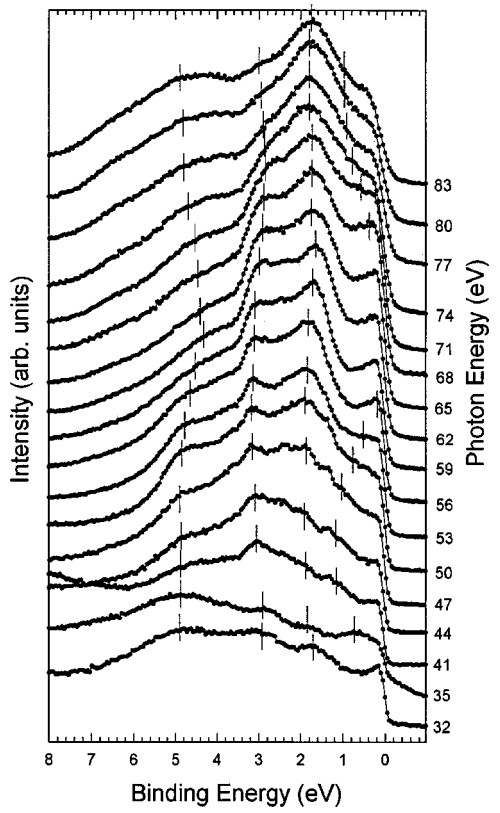

FIG. 2. The photoemission spectra taken at normal emission ($k_{\|}=0$) for photon energies 30–83 eV.

The experimentally determined[22] crossing of E_F by surface bands at about midway along $\bar{\Gamma}$-$\bar{X}$ is evident also in the calculated band structure presented in Fig. 4. Here the experiment and the theory are in a good agreement with regard to placing the crossing of E_F at $0.45\pm0.03\,\bar{\Gamma}$-$\bar{X}$ (experiment[22]) and $0.43\pm0.03\,\bar{\Gamma}$-$\bar{X}$ (calculation), respectively. It is worth noting that the photoemission (ARPES) and IPES data are found to belong to different bands, thus explaining why in the experiment these data are discontinuous at E_F. This is not the effect of limited experimental resolution as suggested previously.[22]

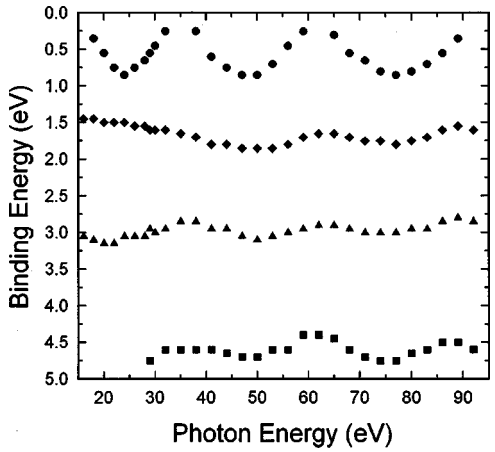

FIG. 3. The experimental band dispersion as a function of photon energy along the $\bar{\Gamma}\langle 112\rangle$ direction ($k_{\|}=0$) adapted from spectra like those shown in Figs. 1 and 2.

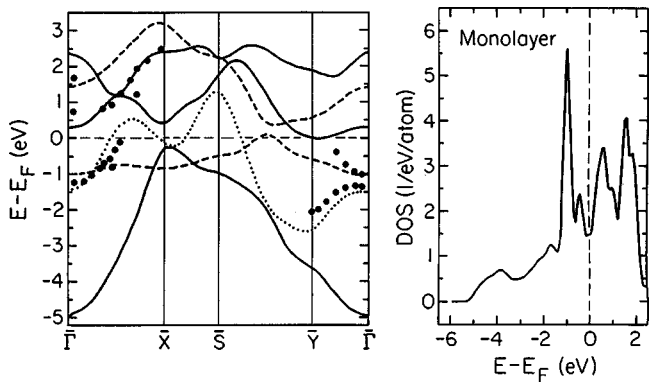

FIG. 4. Surface bands (left) and DOS (right) calculated for the Mo(112) monolayer. Solid curves are the bands that have the *z*-reflection (even) symmetry while dashed lines are the odd states. PES and IPES data for surface-sensitive states [McAvoy *et al.* (Ref. 22)] are represented with symbols.

The symmetries of the surface resonances at normal emission ($\bar{\Gamma}$) have been assigned on the basis of the light-incidence angle dependence of the photoemission spectra[22] and can be compared with our theoretical symmetry assignments. The surface resonance at approximately 3.1 and the bulk band at 2.4 eV are enhanced with a light-incidence angle of 45° and suppressed with a light-incidence angle of 70°. For the band with about 1 eV binding energy at $\bar{\Gamma}$ [dispersing towards the Fermi level at $0.45\,(\bar{\Gamma}$-$\bar{X})$], the intensity is enhanced with light at 70° light-incidence angle. Since light from the synchrotron is highly plane polarized, the more normal the light-incidence angle, the more *s*-polarization and the more vector potential A of the incident light lies parallel to the surface. Since, at $\bar{\Gamma}$ the point group symmetry is C_{2v}, the bands observed in photoemission must be $a_1\,(s,p_z,d_{3z^2-r^2})$, $b_1\,(p_x,d_{xz})$, or $b_2\,(p_y,d_{y2})$. The enhancement of the approximately 3.1-eV surface resonance in more *s*-polarized light indicates that these bands are b_1 or b_2 symmetry. The enhancement of the bands near E_F with increasing vector potential along the surface normal (greater light-incidence angles) indicates that these bands are a_1 symmetry in character. This symmetry assignment, derived by angle-resolved photoemission, also is in agreement with results of the calculations for the real-space distribution of electron density for the Mo(112) monolayer. As seen in Fig. 5 (upper panel), the calculated symmetry of this occupied state at -1.5 eV at $\bar{\Gamma}$ (with the band mapping plotted in Fig. 4) is of a_1 symmetry and largely $d_{3z^2-r^2}$ in character, consistent with experiment.

We also note that there must be a state of b_2 (odd) symmetry (p_y,d_{yz}) to provide the dispersion of a sigma-type band along $\bar{\Gamma}$-$\bar{Y}$ as reported elsewhere.[22] The bottom of this band is at about 1 eV binding energy at $\bar{\Gamma}$ (Ref. 22) and the band dispersion is also plotted in Fig. 4. This band would tend to diminish the enhancement of the bands near E_F in *p*-polarized light. This odd symmetry band is recovered in our theoretical band structure as well (Fig. 5, bottom panel).

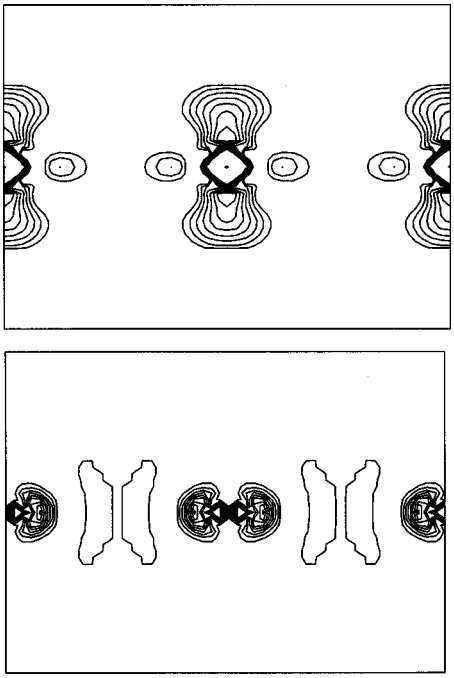

FIG. 5. The real-space distribution of electron density for the Mo(112) monolayer. Upper panel: The even state (−1.5 eV at Γ) shows the a_1 symmetry and largely $d_{3z^2-r^2}$ character. Bottom panel: The odd surface state (−1.4 eV at Γ). The horizontal axis is along the atomic row of the Mo(112) monolayer (which corresponds to the ⟨111⟩ direction, with Mo atom separation of 2.73 Å), the vertical, along the normal to the surface. The contour separation is 0.01 electron/unit cell, the cutoff is 0.1.

In spite of being a rather over idealized model, a single Mo(112) monolayer can reproduce the important features of the surface electronic structure of the Mo(112). However, the lower-surface-sensitive state (−3.1 eV), also found in the photoemission[22] cannot be treated by the monolayer model. Indeed, in the calculated DOS there is no corresponding peak at this energy (see Fig. 4, right panel). Presumably, this state may be attributed to back- and side-bonding electrons, while the upper band (the state near the Fermi level), to the electrons leaking into vacuum, which may not be so sensitive to the substrate.

To verify the above limitations of the monolayer-model calculations, we have performed calculation of the bands and the density of states (Fig. 6) within the model that includes the subsurface layer, that is, for the three-layer slab. Aiming for a qualitative description, the unit cell has been slightly transformed to gain the central symmetry essential for such calculations. Apart from certain quantitative differences (e.g., in the width of occupied part of the valence band) between the calculated band structures for the three-layer slab (Fig. 6) and for one monolayer (see Fig. 4), agreement with experimental dispersion of the surface bands near the Fermi level is, again, rather good. As seen in the right panel of Fig. 6, the inclusion of the subsurface layer leads to a peak in the density of states at −3.2 eV, absent in the density of states calculated for the monolayer (see the right panel of Fig. 4). This lower-surface resonance band at 3.2 eV still appears to have originated from the bonding electrons in the surface region: due to the open structure of the Mo(112) face, the second layer indeed is a part of the surface, and the feature is partly surface in origin.

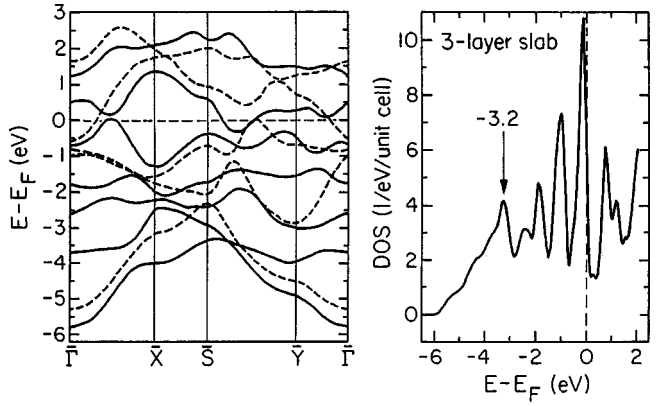

FIG. 6. Surface band structure (left) and DOS (right) for the three-layer Mo(112) slab. Solid curves are the bands that have the *z*-reflection (even) symmetry while dashed lines are the odd states. Note the rise of the peak at −3.2 eV that indicates partly a surface origin of corresponding peak in the normal photoemission spectra shown in Figs. 1 and 2.

IV. BULK Mo BAND STRUCTURE ALONG ⟨112⟩ AND PERTURBATIONS IN PHOTOEMISSION

Since the spectra presented in Figs. 1 and 2 are taken for normal emission or $k_{\parallel}=0$, the peaks exhibiting photon-energy dependence (Fig. 3) can be attributed to the bulk bands dispersing with $k_{\perp}$. In particular, the states at about 4.3 and 2.4 eV are clearly bulk bands. As discussed elsewhere,[22] inspite of bulklike dispersion ranging from 0.3 to 1.0 eV depending upon photon energy, the state at 0.7 eV may, nonetheless, retain some surface character as indicated by the sensitivity of this state to contamination.

The calculated bulk bands and related one-dimensional DOS along the ⟨112⟩ direction (Fig. 7) are shown in Fig. 8. There is a qualitative agreement between experimentally found dispersion of the main peaks that we assign to the bulk induced features (see Fig. 3) and calculated dispersion for occupied bands (Fig. 8). In particular, behavior of the peak at 0.3–1.0 eV binding energy in the normal photoemission spectra can be directly attributed to the Fermi level crossing of the band at about 21% along the Brillouin zone edge (0.26

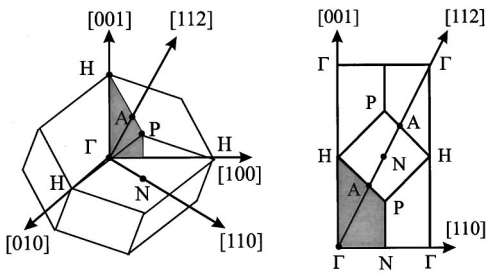

FIG. 7. The ⟨112⟩ direction in the bulk Brillouin zone (BZ) for Mo (left) and its position within the (110) plane (right). The shadowed portion is the part of the (110) plane within the first BZ.

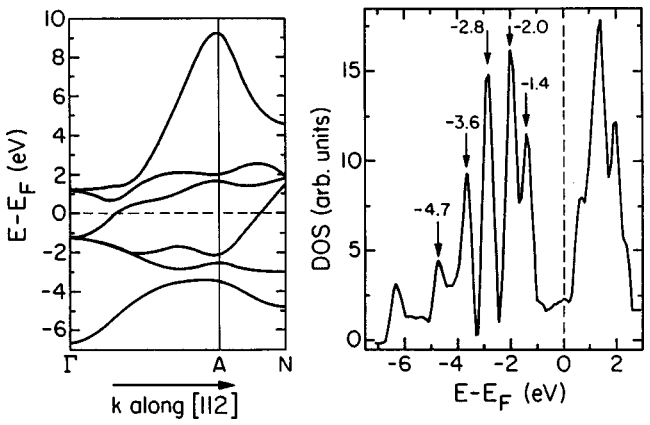

FIG. 8. Calculated bulk bands (left) and DOS (right) along the along the ⟨112⟩ direction.

$Å^{-1}$ in the first Brillouin zone going from Γ to *A*, see Figs. 7 and 8). The Fermi level crossing in Fig. 3, at 15 eV, is consistent with the calculated critical point of 2.7 $Å^{-1}$ (or 0.26 $Å^{-1}$ in the first Brillouin zone). From this value we can estimate the inner potential of 12.9 eV or a band width of 8.3 eV if the work function is close to the calculated value of 4.6 eV. The apparent Fermi level crossing at 64 eV matches with the calculated value of 4.62 $Å^{-1}$ (or again 0.26 $Å^{-1}$ in the first Brillouin zone), while matching 91 eV with the critical point 5.14 $Å^{-1}$ (or again 0.26 $Å^{-1}$ in the first Brillouin zone) provides an estimated inner potential of 17.4 and 11.8 eV (i.e., band widths of 12.8 and 5.2 eV), respectively. The average estimate of the inner potential is 13.4 eV or a bandwidth 8.8 ± 3 eV, which is a little higher than our calculation of the bandwidth (6.7 eV) but still reasonable. Exact determination of the critical points is limited by the finite resolution of our spectrometer (150–250 meV in the range of photon energies plotted in Figs. 1 and 2).

Surprising variations in the experimental inner potential with kinetic energy are also known from dynamical LEED scattering.[44] The inner potential for molybdenum (100) derived from LEED (Ref. 49) was seen to vary from 18 eV (0–40 eV electron kinetic energies) to about 14 eV (above 80 eV electron kinetic energy). It appears that in photoemission, like in LEED, the experimental inner potential also generally falls with increasing kinetic energy. While our values of the inner potential are smaller than those derived from LEED [for the (100) surface], our values remain larger than those expected from theory.

It should be noted, however, that the above straightforward interpretation of the photon-energy dependent spectra, based on implied validity of the bulk *k*-conserving transitions, fails in explaining the apparent Fermi level crossing at 34 eV, which gives the critical point 3.53 $Å^{-1}$ (or 0.109 $Å^{-1}$ in the first Brillouin zone). This is absent in the calculated band structure (see Fig. 8). Moreover, at least one band (at about 1.5 eV binding energy) is insensitive to this Fermi level crossing. Therefore other possible factors such as plasmon excitations, in particular, harmonics of the surface plasmon or multipole resonance should unavoidably be included in modeling the experimental band structure, as discussed below. Final-state effects must be considered as well because this photon energy is very close to the super Coster-Kronig resonant photoemission involving the $4p_{3/2}$ to $4d$ excitation with a threshold of 35.5 eV.

Obviously, just near the surface, the $k_\perp$-selection rules are no longer strictly valid, so one might expect strong absorption effected mainly by indirect transitions from the conduction bands into the unoccupied *d* bands. In this region, position and intensity of the peaks in photoelectron spectra are determined by the density of states. Indeed, the position of the main peaks photoemission spectra for Mo(112) along wave-vector direction of the surface normal (Figs. 1 and 2) show a qualitative correspondence to the calculated one-dimensional distribution of initial states (Fig. 8). Identification of all the bands by means of comparison with the bulk band structure along the surface normal is one key to understanding the origin of the photoemission peaks, but cannot be used exclusively.

The photoemission intensity should also depend on the density of states at the final electron energy.[50] Thus, when the final energy of the electrons excited from their initial states below Fermi level occurs in the region of low DOS (or in the gap that could arise from the spin-orbit coupling as reported for tungsten,[51]) the related peak in the photoemission spectra might be essentially damped. Assuming the final state as bulk-like and the matrix elements for the transitions to be independent of energy (which has been shown to be a rather good approximation in most cases[50,52–55]) the corresponding changes in the spectral intensity can be qualitatively evaluated within a simple model for absorption of the impinging light. Then, for arbitrary excitation $\hbar\omega$, the intensity of photoemission can be evaluated simply as the product of the densities of initial and final states, that is,

$$l(E_i,\omega) \sim n(E_i)n(E_i+\hbar\omega). \tag{3}$$

The $k_\parallel$ conservation leads to the situation where only the changes in the density of states $n(E)$ along the ⟨112⟩ direction (Fig. 8) are important for the normal photoemission. While the calculated intensities of normal photoemission spectra for various photon energies (using the DOS calculated for the extended energy range) provide a qualitatively correct description of the peak positions, the calculated spectra do not agree well with those experimentally observed. It is found that the agreement can be substantially improved by including contributions from the surface as well.

To account for the enhanced yield from the surface, Eq. (3) has also been applied to treat the $k_\parallel = 0$ spectra for the three-layer slab at Γ. Then, a ''surface-induced'' fraction can be added to the bulk-induced calculated spectra to attain the best available fit to the shape of the experimental photoemission spectra (Fig. 9). The ''degree'' of the required surface-induced part has been found dramatically dependent on the photon energy. In particular, for the light energy of 20 eV, the surface photoemission yield is found to be five times greater than that needed to fit to the spectra for 24 eV. The strong surface character of photoemission at 20 eV is suppressed in favor of more bulk-induced (bulklike) photoemission at the photon energy of 24 eV, which is about the energy of volume plasmon in Mo.[56–59]

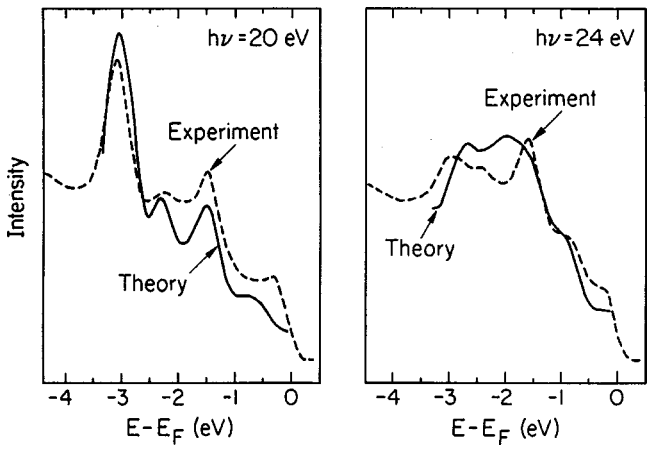

FIG. 9. Simulation of the normal photoemission spectra for two characteristic photon energies that correspond to the surface resonance (20 eV) and the bulk plasmon energy (24 eV). The surface yield, required to attain the best fit to the shape of the spectra (shown by dashed line), for 20 eV photon energy is five times greater than that for 24 eV.

V. DISCUSSION: THE ORIGIN OF THE PEAKS IN THE PHOTOEMISSION SPECTRA FOR THE Mo(112)

The results of ARPES studies for the Mo(112) surface can be summarized as follows: (i) The peaks are sensitive to contamination, but to somewhat different degrees depending on the band and wave vector. For example, oxygen adsorption leads to a decrease in heights and sharpness of the peaks at about 3.0 eV and about 1 eV binding energy.[22,60] (ii) For the normal photoemission, i.e., zero parallel wave vector of outgoing electrons ($k_{\|}=0$), the main peak positions noticeably changes on increasing energy, consistent with bulk band structure for the most part. (iii) These photoemission features result in a sharp change of the spectral shape within a narrow energy interval of about 24 eV (see Fig. 1).

Under proper conditions, the photoemission current from metal surfaces is determined mainly by the yield from the surface.[7,8,11,61] When the energy of the impinging light is lower than the bulk plasmon energy, the light may be absorbed just in the surface region thus exciting the electrons that give rise to the photoemission. It is a nonlocal response near the metal surface that makes the second term in the matrix elements in Eq. (3) nonzero. A detailed description of induced-electromagnetic fields near the surface (suggested by Feibelman[6] from a sophisticated microscopical random-phase approximation/local-density approximation approach and assuming a jellium model) was supported by photoemission study of simple metal surfaces and thin films (for a review see Refs. 8 and 16).

It has been recently recognized that the surface photoeffect intimately relates to excitation and subsequent decay of so-called multipole surface plasmons. Having an oscillating electrostatic field normal to the surface, this mode, in contrast to a ''regular'' surface plasmon, can be excited directly by incident photons, i.e., it is strongly dipole active.[8,16] The multipole mode of collective excitations is extremely localized within the surface region so that its energy, which is usually about 0.6–0.8 fraction of the bulk plasmon energy, is roughly determined by a local electronic density at the surface.[6,8,16]

The multipole modes have been directly observed by electron energy-loss spectroscopy (EELS) for surfaces of simple metals. For transition metals, a strong decay of the plasmons due to a high density of states provided by the *d*-bands make the EELS spectra too involved to detect the multipole-modes unambiguously. Thus it is not surprising that to date the surface photoeffect has not yet been observed for transition-metal surfaces.

Nonetheless, photoelectrons—electrons resulting from decay of the multipole mode—can give rise to a resonance in the surface-photoemission intensities, thus, for the photon energies close to multipole mode, the photoemission signal is dominated by the density of states at the surface.[8,16] For energies corresponding to the excitation of bulk plasmons, photoemission has a more bulk-like origin.[8,16] This provides the key to understanding the behavior of the photon-energy dependence of the photoemission peaks in the Mo(112) spectra. Recall that the characteristic loss values for Mo include two volume plasmons at 24.4 and 10.4 eV,[58–61] two surface plasmons at 14.8 eV (Refs. 58 and 62) and 9.5 eV,[58–61] and another surface mode at about 19 eV (Refs. 58 and 62) that, evidently, can be attributed to multipole mode.

One may expect a sharp redistribution between the surface and the bulk yields, in photoemission, within the region of resonant excitation of multipole mode and bulk plasmons, respectively, which is clearly seen in experimental spectra (see Fig. 1) and further illustrated by estimation of relative yields shown in Fig. 9. In particular, we suggest that each peak combines the surface and the bulk yields in essence from two photoemission peaks closely spaced but unresolved. Then, due to the surface photoeffect, their relative participation will change with photon energy, which can appear in the spectra as a shift of the peak binding energies, namely, having a surface peak at -0.3 eV and a wide bulk peak at -1 eV, under conditions of optimal surface enhancement (say at 16–20 eV photon energy), we would see the photoemission ''peak'' close to E_F, while the peak binding energy increases to -1 eV at the plasmon energy 24 eV.

The most challenging feature of the normal photoemission spectra for Mo(112) is the periodic oscillations of the positions of the peaks with increasing photon energy, clearly evident from the dispersion plots in Fig. 3. These oscillations are most pronounced for the photoemission band near the Fermi energy but are noticeable for the other bands as well. The period can be revealed by the positions of the minima in the upper band (24, 48, 74 eV) and again, are multiples of about 24 eV. The explanation of the behavior of the bands is straightforward provided that the photon can cause excitation of two, three, and more plasmons (presumably, involving certain virtual states at intermediate steps of the process). Then enhancement and following drop of the surface photoemission will become periodic in photon energy thus resulting in the redistribution between the surface and the bulk yeilds, which in turn, will be observed as shifts in spectral peaks. This shift is evident for the occupied band near E_F because of substantial difference in positions of the surface

and the bulk peaks, while for the lower bands these peaks are rather close to each other, so the shifts are not as pronounced.

VI. CONCLUSIONS

Many experimental observations derived from the photoelectron spectra for the Mo(112) such as band dispersion, Fermi level crossings, and symmetry assignments of the surface states can be explained in terms of the surface and the bulk band structure. In particular, the symmetry of the state at the surface Brillouin zone center, about 1–1.5 eV binding energy, are found to have a_1 symmetry in both experiment and theory, while the band along $\bar{\Gamma}$-$\bar{Y}$ at about 0.8 eV binding energy is found to be odd with respect to the $\bar{\Gamma}$-$\bar{Y}$ mirror plane in both experiment and theory.

From a comparison of the calculated bulk band structure and the experimental data, we find that the band width of Mo(112) is about 6.7 eV (theory) and 8.8 eV (experiment). Taking into account the derived inner potential, we can match the bulk band structure with the experimental data. Corrections in the spectral intensities due to plasmon resonances are indicated nonetheless, though future photoemission yield calculations should take into account the light polarization and the different surface and bulk Debye temperatures.[62]

ACKNOWLEDGMENTS

This work was supported by NSF through Grant No. DMR-98-02116, the Center for Materials Research and Analysis (CMRA) and the Nebraska Research Initiative at the University of Nebraska, and the North Atlantic Treaty Organization (NATO) under Grant No. PST.CLG.976845. The authors would like to thank D. McIlroy, T. Komesu, G. Katrich, T. (nee McAvoy) Rybnicek, and C. Waldfried for their assistance in the measurements. Portions of this work were carried out at the Synchroton Radiation Center, Stoughton, Wisconsin, which is funded by the NSF.

[1] L. I. Schiff and I. H. Thomas, Phys. Rev. **47**, 860 (1935).
[2] R. E. B. Makinson, Proc. R. Soc. London, Ser. A **162**, 367 (1937).
[3] C. Schwartz and W. L. Schaich, Phys. Rev. B **30**, 1059 (1984).
[4] K. Kempa and R. Gerhards, Solid State Commun. **53**, 579 (1985).
[5] K. L. Kleiwer, in *Photoemission and the Electronic Properties of Surfaces*, edited by B. Feuerbacher, A. Fitton, and R. F. Willis (Wiley, New York, 1978), p. 540.
[6] P. J. Feibelman, Prog. Surf. Sci. **12**, 287 (1982).
[7] P. A. Dowben, Surf. Sci. Rep. **6–8**, 151 (2000).
[8] A. Liebsch, Phys. Rev. Lett. **67**, 2858 (1991); *Electronic Excitations a Metal Surfaces* (Plenum, New York, 1997).
[9] K.-D. Tsuei, E. W. Plummer, A. Liebsch, K. Kempa, and P. Bakshi, Phys. Rev. Lett. **64**, 44 (1990).
[10] R. T. Sprunger, G. M. Watson, and E. W. Plummer, Surf. Sci. **269/270**, 551 (1992).
[11] E. W. Plummer, Solid State Commun. **84**, 143 (1992).
[12] M. Rocca, Surf. Sci. Rep. **22**, 1 (1995).
[13] Bong-Ok Kim, Geunseop Lee, E. W. Plummer, P. A. Dowben, and A. Liebsch, Phys. Rev. B **52**, 6057 (1995).
[14] H. J. Levinson, E. W. Plummer, and P. J. Feibelman, Phys. Rev. Lett. **43**, 952 (1979); J. A. Gaspar, A. G. Eguiluz, K.-D. Tsuei, and E. W. Plummer, *ibid.* **67**, 2854 (1991).
[15] I. N. Yakovkin, G. A. Katrich, A. T. Loburets, Yu. S. Vedula, and A. G. Naumovets, Prog. Surf. Sci. **59**, 355 (1998); P. Apel, Phys. Scr. **25**, 57 (1982).
[16] E. W. Plummer and W. Eberhard, Adv. Chem. Phys. **49**, 533 (1982).
[17] K. E. Smith, Annu. Rep. Prog. Chem., Sect. C: Phys. Chem. **92**, 253 (1997).
[18] E. W. Plummer and P. A. Dowben, Prog. Surf. Sci. **42**, 201 (1993).
[19] D. Westphal and A. Goldmann, Surf. Sci. **126**, 253 (1983).
[20] A. Goldmann, Surf. Sci. **178**, 210 (1986).
[21] K. Desinger, W. Altmann, and V. Dose, Surf. Sci. **201**, L491 (1988).
[22] T. McAvoy, J. Zhang, C. Waldfried, D. N. McIlroy, P. A. Dowben, O. Zeybek, T. Bertrams, and S. D. Barrett, Eur. Phys. J. B **14**, 747 (2000).
[23] K. S. Shin, C. Y. Kim, H. W. Kim, J. W. Chung, S. K. Lee, C. Y. Park, S. C. Hong, T. Kinoshita, M. Watanabe, A. Kakizaki, and T. Ishii, Phys. Rev. B **47**, 13 594 (1993).
[24] J. W. Chung, in *Electronic Surface and Interface States on Metallic Systems*, edited by E. Bertel, and M. Donath (World Scientific, Singapore, 1995), p. 67.
[25] J. W. Chung, K. S. Shin, and S. C. Hong, Mod. Phys. Lett. B **21**, 865 (1993).
[26] J. W. Chung, Appl. Surf. Sci. **113/114**, 436 (1997).
[27] H. K. S. Shin, H. W. Kim, J. W. Chung, Surf. Sci. **385**, L978 (1997).
[28] E. Tosatti, in *Electronic Surface and Interface States on Metallic Systems*, edited by E. Bertel and M. Donath (World Scientific, Singapore, 1995), p. 67.
[29] T. E. Felter, R. A. Barker, and P. J. Estrup, Phys. Rev. Lett. **38**, 1138 (1977).
[30] A. Fasolino and E. Tosatti, Phys. Rev. B **35**, 4264 (1987).
[31] A. Fasolino, G. Santoro, and E. Tosatti, Surf. Sci. **125**, 317 (1983).
[32] K. Smith and S. Kevan, Phys. Rev. B **43**, 3986 (1991).
[33] K. Smith and S. Kevan, Phys. Rev. B **45**, 13 642 (1992).
[34] J. C. Campuzano, J. E. Ingesfield, D. A. King, and C. Somerton, J. Phys. C **14**, 3099 (1988).
[35] K. E. Smith, G. S. Elliot, and S. D. Kevan, Phys. Rev. B **42**, 5385 (1990).
[36] S. L. Weng, E. W. Plummer, and T. Gustafsson, Phys. Rev. B **18**, 1718 (1978).
[37] G. P. Kerker, K. M. Ho, and M. L. Cohen, Phys. Rev. B **18**, 5473 (1978).
[38] R. C. Cinti, E. al Khoury, B. K. Chakraverty, and N. E. Chris-

tensen, Phys. Rev. B **14**, 3296 (1976).
[39] C. Noguera, D. Spanjaard, and D. W. Jepsen, Phys. Rev. B **17**, 607 (1978).
[40] P. Soukasian, R. Rivan, J. Lecante, E. Wimmer, S. R. Chubb, and A. J. Freeman, Phys. Rev. B **31**, 4911 (1985).
[41] S. R. Chubb, E. Wimmer, A. J. Freeman, J. R. Hiskes, and A. M. Karo, Phys. Rev. B **36**, 4112 (1987).
[42] Takashi Komesu, C. Waldfried, Hae-Kjung Jeong, D. P. Pappas, T. Rammer, M. E. Johnston, T. J. Gay, and P. A. Dowben, Proc. SPIE **3945**, 6 (2000).
[43] P. A. Dowben, D. LaGraffe, and M. Onellion, J. Phys.: Condens. Matter **1**, 6571 (1989).
[44] L. J. Clarke, *Surface Crystallography: An Introduction to Low Energy Electron Diffraction* (Wiley, New York, 1985).
[45] H. Krakauer, M. Posternak, and A.-J. Freeman, Phys. Rev. B **19**, 1706 (1979).
[46] M. Posternak, H. Krakauer, A. J. Freeman, and D. D. Koelling, Phys. Rev. B **21**, 5601 (1980).
[47] A. J. Freeman, M. Weinert, and E. Wimmer, Phys. Rev. B **28**, 593 (1983).
[48] O. Jepsen, J. Madsen, and O. K. Andersen, Phys. Rev. B **18**, 605 (1978).
[49] L. J. Clarke and L. Morales de la Garza, Surf. Sci. **99**, 419 (1980).
[50] I. Petroff and C. R. Vishwanathan, Phys. Rev. B **4**, 799 (1971).
[51] R. F. Willis and N. E. Christensen, Phys. Rev. B **18**, 5140 (1978).
[52] N. R. Avery, Surf. Sci. **111**, 358 (1981).
[53] T. L. Loucks, Phys. Rev. **139**, A1181 (1965).
[54] H. J. F. Jansen, W. E. Krolikowski, and W. E. Spicer, Phys. Rev. B **1**, 478 (1970).
[55] I. N. Yakovkin, Surf. Sci. **442**, 431 (1999).
[56] J. H. Weaver, D. W. Lynch, and C. G. Olson, Phys. Rev. B **10**, 501 (1974).
[57] G. A. Katrich, V. V. Klimov, N. V. Petrova, and I. N. Yakovkin, Izvestiya Russ. Ac. Sci., Ser. Phys. **58**, 7 (1994).
[58] G. A. Katrich, V. V. Klimov, and I. N. Yakovkin, J. Electron Spectrosc. Relat. Phenom. **68**, 369 (1994).
[59] G. A. Katrich, V. V. Klimov, and I. N. Yakovkin, Ukr. J. Phys. **37**, 429 (1992).
[60] C. Waldfried, D. N. McIlroy, J. Zhang, P. A. Dowben, G. A. Katrich, and E. W. Plummer, Surf. Sci. **363**, 296 (1996).
[61] G. A. Katrich and I. N. Yakovkin, Ukr. J. Phys. **38**, 93 (1993).
[62] Y. Ballu, J. Lecante, and H. Rousseau, Phys. Rev. B **14**, 3201 (1976).